Int. J. Electrochem. Sci., 16 **(2021)** Article ID: 210935, doi: 10.20964/2021.09.44

International Journal of
ELECTROCHEMICAL
SCIENCE
www.electrochemsci.org

Hydroxypropyl Methylcellulose Phthalate Biopolymer as an Anticorrosion Coating

Shih-Chen Shi

Department of Mechanical Engineering, National Cheng Kung University (NCKU), No.1 University Road, Tainan 70101, Taiwan
E-mail: scshi@mail.ncku.edu.tw

Received: 6 February 2018 / *Accepted:* 20 July 2021 / *Published:* 10 August 2021

This study involved a carbohydrate material: hydroxypropyl methyl-cellulose phthalate (HPMCP), a derivative of the biopolymer hydroxypropyl methylcellulose. It is a biodegradable and environmentally friendly material. This study tested the durability and corrosion resistance of HPMCP coatings on high-speed steel in solutions with different pH values and different immersion durations. The electrochemical tests included potentiodynamic polarization and electrochemical impedance spectroscopy. Water channels formed as the coating dissolved in an acidic environment, which degraded its corrosion resistance. However, with prolonged immersion, the corrosion resistance of the system was maintained because iron oxides and chromium oxides were generated between the HPMCP coating and high-speed steel. The corrosion resistance mechanism of HPMCP coatings is proposed and discussed.

Keywords: biopolymer; HPMCP; potentiodynamic polarization; EIS

1. INTRODUCTION

Early anticorrosion measures generally involved the alloying of metals for cathodic protection or applying or applying a coating of sacrificial metal on the surface. In recent years, as a result of cost issues, many researchers have resorted to high molecular weight (HMW) polymers as a new anti-corrosion material because of their excellent anti-corrosion properties and comparatively low costs. However, HMW polymers also pose certain environmental risks because they can be difficult to degrade in nature. The use of environment-friendly polymers has become a new trend due to the rise of green awareness and the emergence of the energy crisis. An example of an environmentally friendly HMW polymer is hydroxypropyl methylcellulose (HPMC), a non-ionic cellulose ether that usually presents as a white powdery solid. HPMC is colorless, odorless, and soluble in water and most polar organic solvents. In most applications, HPMC is dissolved in an ethanol-water solution at an appropriate ratio. HPMC has

excellent film-forming and thickening properties and is non-toxic [1, 2]. Thus, it is commonly used in drug manufacture and the food industry [3-5]. In pharmaceutical applications, HPMC can be used as a filler or excipient for oral drugs to assist in drug delivery [6, 7] or act as a medical lubricant [8]. HPMC can also be used as a coating material for controlled drug release [3]. Recently, HPMC has also become the focus of applied research in the mechanical domain [9, 10], with examples including studies on self-repair [11] and tribological performance [12-14]. This study investigated the electrochemical properties of hydroxypropyl methylcellulose phthalate (HPMCP), a derivative of hydroxypropyl methylcellulose (HPMC). HPMCP is formed by adding phthalates to HPMC, which alters the functional groups of HPMC and enhances its endurance in acidic environments.

The use of polymers as a protective coating on metal will isolate it from the corrosive environment preventing direct contact between the base metal and its environment, which is suitable for various applications. Although the lack of metallic elements in these coatings will help conserve limited resources, certain polymers still pose a significant threat to the environment. These polymers are also difficult to degrade in the natural environment [15, 16]. Therefore, to realize a green anti-corrosion coating, HPMCP, a biodegradable and environmentally friendly material that can provide an appropriate level of corrosion resistance. Because HPMC is soluble in water, in previous studies, it was usually added as an anticorrosion agent to reduce the corrosive effects of a working environment solution [16-19]. Nonetheless, for sustainable development, replacing solution-based anticorrosion measures with solid coatings is a safer option for the environment[20, 21]. HPMCP was used in this study because it retains the film formability of HPMC, and its films are highly insoluble in water and acidic environments. In addition, HPMCP films are chemically stable [22, 23]. Therefore, HPMCP has a higher potential than HPMC for this application.

2. EXPERIMENTAL

2.1. HPMCP Film Preparation

First, 80 mL of ethanol was mixed with 20 mL of pure water, 10 g of HPMCP (HP-50, Shin-Etsu, Tokyo, Japan) powder was added to this mixture and stirred using a hotplate magnetic stirrer until it was completely dissolved to form the HPMCP solution. Finally, 600 μL of the resulting mixture was pipetted and dropped onto a high-speed steel (HSS) sample (JIS, SKH51), and the coated sample was placed in a dry vacuum box for 12 h. This procedure was repeated thrice to prepare the HPMCP coating. The film thickness was controlled at 600 ± 25 μm [24].

2.2. Electrochemical Properties of HCMPC coatings

The liquids for the corrosive environment were prepared using NaCl solution, and the pH was adjusted using an HCl solution from pH3 to pH7.

The electrochemical characteristics of the coating were studied using potentiodynamic polarization analysis (ECW-5000, Taichung, Taiwan) over a scanning range of −1000 to +500 mV at a scan rate of 1 mV/s. Electrochemical impedance spectroscopy (EIS; HIOKI 3533-05, Taichung, Taiwan) was performed in the scanning frequency range of 200 kHz–0.1 Hz with a signal amplitude perturbation of 0.02 V. Ten points were recorded at frequencies in multiples of ten. The test pieces were immersed in different pH solutions for various times (2, 4, 8, 16, and 24 h) before the tests.

2.3. Thickness Measurements

The thickness was measured using an external micrometer. The substrate thickness was first measured before being coated and then counted again after the coating was prepared. The final thickness measurement was taken after soaking the coated substrate in the corrosive solution for 24 h, thus obtaining the coating thicknesses before and after the corrosion experiment.

2.4. Raman Spectroscopy and Fourier Transform Infrared Spectroscopy Analyses

In this experiment, Raman spectroscopy and Fourier transform infrared (FTIR) spectroscopy were performed to determine whether new components were formed between the HPMCP coating and the HSS sample after corrosion. Since Raman and FTIR spectroscopies only analyze the sample surface, the coating and HSS steel samples were separated before this experiment, and then the separated HSS sample was analyzed.

3. RESULTS AND DISCUSSION

3.1. Potentiodynamic Polarization Analysis

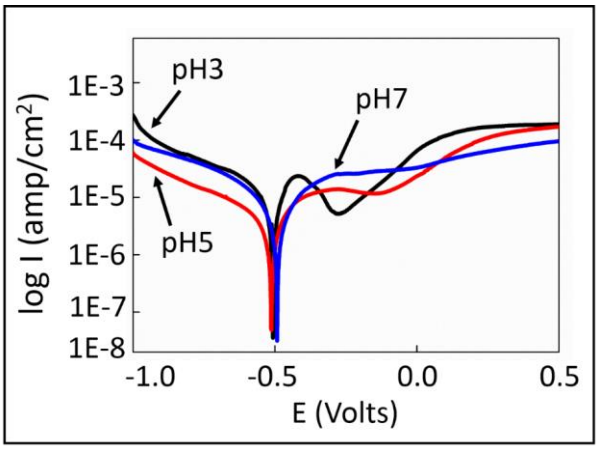

Figure 1. Polarization curves of HPMCP coating under different pH values

Figure 1 illustrates the polarization curves of the HPMCP coating in corrosive solutions with different pH values. The lowest point on the curve indicates the corrosion potential (E_{corr}). The corrosion

current (I_{corr}) can be obtained using the Tafel extrapolation method. I_{corr} is considered as an indicator of corrosion resistance, with a lower value of I_{corr}, indicating better corrosion resistance.

As listed in Table 1, I_{corr} increases with decreasing pH, which indicates that highly acidic environmental solutions will damage the HPMCP coating. The anticorrosion behavior measured by potentiodynamic polarization was considered to be a real-time characteristic. To investigate the effects of prolonged immersion on the corrosion resistance of a coating and the underlying mechanisms of these effects, an analysis using electrochemical impedance spectroscopy (EIS) was necessary.

Table 1. Fitting results obtained from Tafel extrapolation for HPMCP coating's polarization curves.

pH value	E_{corr} (V)	I_{corr} (A/cm^2)	βa (mV/dec)	βa (mV/dec)
7	-0.238	5.2×10^{-6}	195	173
5	-0.438	5.7×10^{-6}	232	438
3	-0.310	1.1×10^{-5}	147	292

3.2. Electrochemical Impedance Spectroscopy Analysis

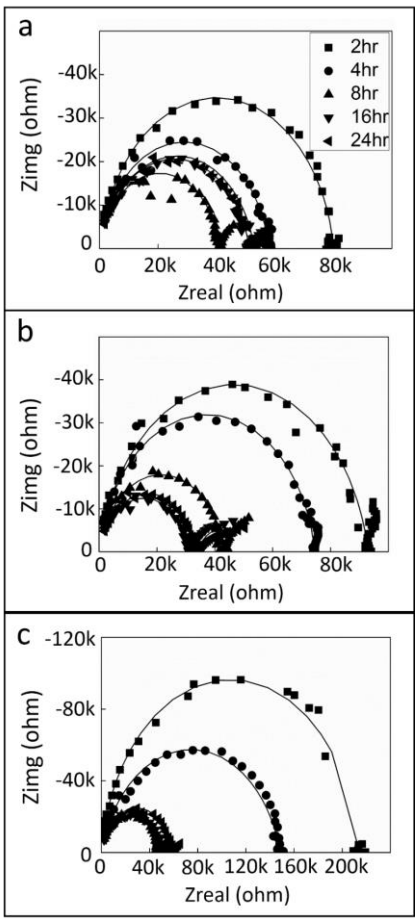

Figure 2. EIS results for HPMCP coatings after immersion in solutions with different pH values for 2–24 h: (a) pH = 3, (b) pH = 5, and (c) pH = 7. (Symbol: experimental data; line: fitting results.)

Figure 2 illustrates the EIS results of the HPMCP coatings immersed in corrosive solutions from pH3 to pH7 values for different durations. As the corresponding Nyquist plots appear as semicircles in the above figure, these data are determined by a time constant. The equivalent circuit model of the coating is shown in Fig. 3.

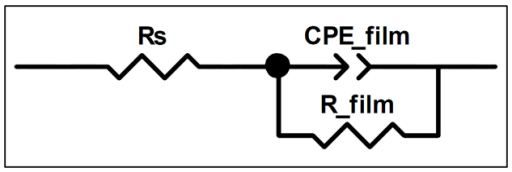

Figure 3. Equivalent circuit model of HPMCP coating

In this figure, 'Rs' is the solution resistance, which refers to the resistance of the corrosive solution between the working electrode and the auxiliary electrode. 'R_film' represents the resistance of the coating, and 'CPE_film' represents the constant phase element, which is similar to the capacitance of the layer. Table 2 lists down the fitting results based on the equivalent circuit model. During the first 2 h, the value of R_film increased with an increase in pH, which verified the results of the PP experiment. This shows that an acidic environment weakens the corrosion resistance of the HPMCP coating. However, after 24 h, the difference between the R_film values corresponding to different pH values was relatively minimal, indicating that the corrosion resistance of the coatings converged to a constant value after prolonged immersion. Besides, a change in R_film over time was observed. Here, it is shown that the R_film value first decreases and then increases slightly for all pH values used in this experiment. The common anticorrosion mechanisms of HMW polymers include path addition [24], reduction of the water content in coatings [25, 26], and the generation of new anti-corrosion substances at the interface [27]. Thickness measurements, volume fraction of water analyses, and Raman surface spectroscopy were performed on HPMCP coatings subjected to different pH values and time parameters to verify the above three potential mechanisms.

Table 2. Results of EIS data fitting by equivalent circuit model.

pH value	Immersion time (h)	R_film (Ω)	CPE_film_T	CPE_film_P
3	2	80071	3.6×10^{-10}	0.910
	4	57839	4.7×10^{-10}	0.990
	8	41037	4.9×10^{-10}	0.892
	16	51134	8.2×10^{-10}	0.865
	24	52818	8.8×10^{-10}	0.864
5	2	92933	5.1×10^{-10}	0.887
	4	74488	4.5×10^{-10}	0.902
	8	42700	5.8×10^{-10}	0.890
	16	30955	9.8×10^{-10}	0.862
	24	33608	1.0×10^{-9}	0.864
7	2	214320	2.1×10^{-10}	0.934
	4	144510	3.1×10^{-10}	0.918
	8	47008	3.1×10^{-10}	0.917
	16	50570	5.0×10^{-10}	0.888
	24	58674	4.9×10^{-10}	0.894

3.3. Changes in Coating Thickness

The thickness of the HPMCP coating was analyzed before and after the test. Here, the relative thickness was used as an indicator to assess the change in film thickness, as follows:

$$\text{Relative Thickness } (\%) = \frac{\text{Coating thickness after corrosion}}{\text{coating thickness before corrosion} \times 100\%} \quad (1)$$

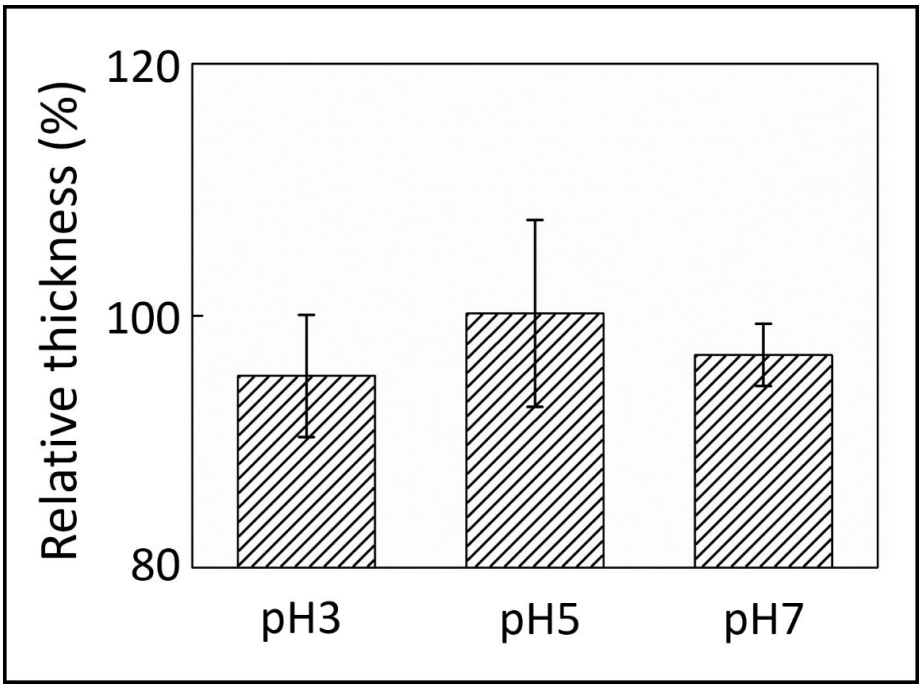

Figure 4. Comparison of relative thicknesses of HPMCP coatings immersed in solutions with different pH values (24 h)

The results are displayed in Figure 4, where it can be observed that the relative thickness of HPMCP at each pH value is less than 100%, indicating that the coating thins over time. Hence, an environmental solution will undoubtedly result in the dissolution of the HPMCP coating.

3.4. Volume Fraction of Water (VFW) Analysis

The volume fraction of water (VFW) refers to the volume of water present within the coating, which indicates the extent of water intrusion from the environment into the layer and the formation of water channels. Hence, this estimation is often considered as an indicator of corrosion resistance. A higher VFW value, is indicative of weak corrosion resistance [25, 26]. Equation 2 was used to analyze the VFW of the coatings based on the EIS results.

$$\text{Volume fraction of water, VFW} = \frac{\log(C_t/C_0)}{\log 80}, \quad (2)$$

where 'C_t' is the coating capacitance after time 't,' and 'C_0' is the coating capacitance at the time t = 0. "80" in the denominator refers to the dielectric constant of water. Since the previously illustrated equivalent circuit model uses a constant phase element (CPE) instead of capacitance 'C,' the CPE has to be converted into an equivalent capacitance [28-32] using Eq. 3, and then substituted into Eq. 2.

$$C = R^{\left(\frac{1-CPE\_film\_P}{CPE\_film\_P}\right)} CPE\_film\_T^{\left(\frac{1}{CPE\_film\_P}\right)}, \quad (3)$$

The results are shown in Fig. 5, where it can be observed that the VFW value increases with an increase in the immersion time. This indicates that the intrusion of water from the environment into the coating has increased with time.

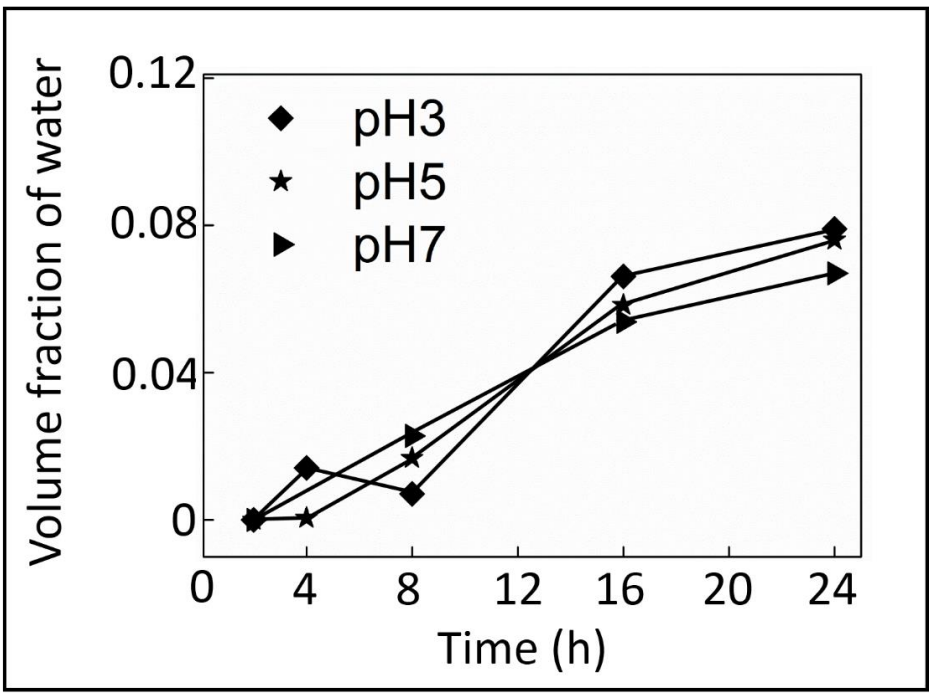

Figure 5. Volume fraction of water analysis results for HPMCP coatings

Upon further analysis, it was found that prolonged immersions yielded very similar VFW results, even with different pH values. This indicated that the water content of the coating had reached saturation, thus stabilizing the corrosion resistance of the layer. Therefore, this evidence and the R_film (24 h) results mutually validated each other.

3.5. Raman and FTIR Spectroscopy Analysis

In a study by Madhankumar et al., a dense iron oxide layer was found on steel surfaces, and the structure of this new layer was different from the loose oxide layer formed by natural corrosion. This dense structure can further strengthen the corrosion resistance characteristics of the material [27]. In this part of the experiment, uncorroded HSS and HPMCP/HSS samples were immersed in the solutions with

pH values of 3, 5, and 7 for 24 h. Raman spectroscopic analysis was then performed on the surface of these HSS samples to determine the generation of new products. The results are illustrated in Fig. 6. Here, 417 cm^{-1} and 577 cm^{-1} peaks correspond to the characteristic peaks of iron oxides [33, 34], which indicate that iron oxides were produced at the interface between the HPMCP coating and HSS.

Further analysis revealed that chromium oxides were also generated on the interface, based on the 530 cm^{-1} peak (black arrow) corresponding to the characteristic signal of chromium oxides. Based on the EIS mapping results, after 24 h of reaction, the R_film value exhibited a rebound instead of a decline, indicating that corrosion-resistant substances were produced on the surface of the HSS. In previous studies, the formation of chromium oxides resulted in good corrosion protection [35, 36]. However, in the Raman spectra shown in Figure 6a, no peak was observed corresponding to chromium oxide, thus excluding this possibility. Arukalam proposed that HPMCP acts as a corrosion inhibitor by adsorbing the metal surface via the aromatic ring and the hydroxypropyl end [16, 37]. Figure 6 (b) shows the FTIR spectra of the HSS surface after the HPMCP/HSS was acid-soaked and the HPMCP coating was removed. The results confirm the adsorption of HPMCP onto the HSS surface. We suggest that the prolonged contact of HPMCP with HSS resulted in an adsorption reaction between the HPMCP and HSS surface, resulting in a thin HPMCP layer that stabilized and maintained the corrosion resistance of the overall system.

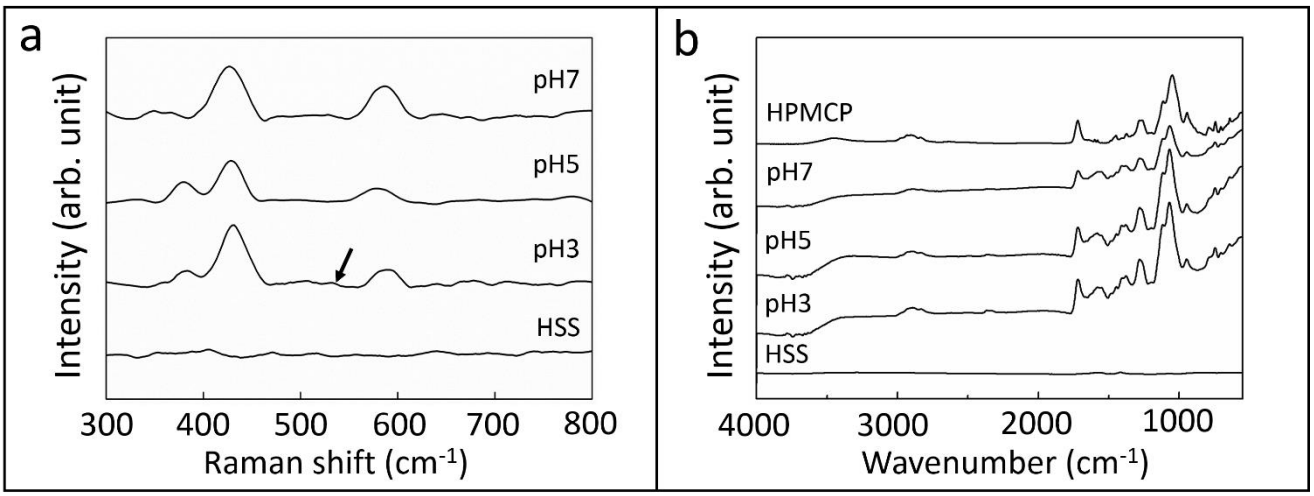

Figure 6. (a) Raman spectra and (b) FTIR spectra of HSS surfaces with corroded HPMCP coatings

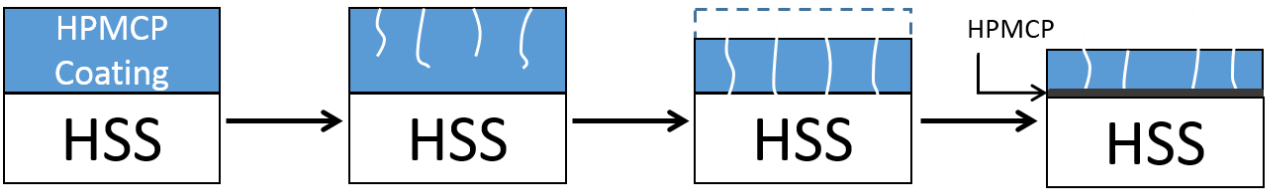

Figure 7. Schematic diagram of anticorrosion mechanism of HPMCP coatings

Based on the results and discussion above, an anticorrosion mechanism for HPMCP coatings was proposed, as shown in Figure 7. This mechanism can be divided into three stages. In the first stage of corrosion, the corrosion resistance decreases over time due to the influx of water from the environment into the coating and the formation of water channels (indicated by white lines). Also, the layer was thinned by corrosion during this process. In the second stage, the high water content causes the water channels to reach the surface of the HSS. The substrate then generates iron oxides as a result of contact with saline solution. In the final stage, the formation of an HPMCP thin layer on the HSS substrate provides a protective effect. Therefore, prolonged immersion will result in the stabilization of the corrosion resistance.

4. CONCLUSIONS

In this study, the electrochemical characteristics of biopolymers immersed in solutions with different pH values were studied, and durability tests were conducted. The conclusions of this study are as follows:

1. In acidic environments, HPMCP can be dissolved to some extent, which reduces its thickness and corrosion resistance.

2. The formation of water channels will gradually reach completion as the immersion time increases, and the environmental fluid will eventually reach the substrate's surface.

3. HPMCP contributes to the adsorption layer on the HSS surface, which improves the durability of its corrosion resistance.

4. The anticorrosion mechanism of HPMCP coatings in acidic environments was established in this work.

ACKNOWLEDGEMENTS
This work was supported by the Ministry of Science and Technology in Taiwan (MOST 109-2221-E-006-046).

References

1. Y. Byun, A. Ward, S. Whiteside, *Food hydrocolloids*, 27 (2012) 364-370.
2. S.C. Shi, F.I. Lu, *Materials*, 9 (2016) 338.
3. D. Zhou, D. Law, J. Reynolds, L. Davis, C. Smith, J.L. Torres, V. Dave, N. Gopinathan, D.T. Hernandez, M.K. Springman, *J. Pharm. Sci.*, 103 (2014) 1664-1672.
4. S.C. Joshi, *Materials*, 4 (2011) 1861-1905.
5. M.E. Bárcenas, C.M. Rosell, *Food Hydrocolloids*, 19 (2005) 1037-1043.
6. J. Siepmann, N. Peppas, *Adv. Drug Delivery Rev.*, 64 (2012) 163-174.
7. J. Siepmann, Y. Karrout, M. Gehrke, F. Penz, F. Siepmann, *Int. J. Pharm.*, 441 (2013) 826-834.
8. C. Chang, L. Zhang, *Carbohydr. Polym.*, 84 (2011) 40-53.
9. S.C. Shi, T.F. Huang, *Opt. Quantum Electron.*, 48 (2016) 532.
10. S.C. Shi, J.Y. Wu, T.F. Huang, *Opt. Quantum Electron.*, 48 (2016) 474.
11. S.C. Shi, T.F. Huang, *Materials*, 10 (2017) 91.

12. S.C. Shi, *Materials*, 9 (2016) 856.
13. S.C. Shi, J.Y. Wu, T.F. Huang, Y.Q. Peng, *Surf. Coat. Technol.*, 303 (2016) 250-255.
14. S.C. Shi, J.Y. Wu, *Smart Sci.*, 5 (2017) 167-172.
15. R. Dong, X. Yan, X. Pang, S. Liu, *Spectrochim. Acta, Part A*, 60 (2004) 557-561.
16. I. Arukalam, I. Madufo, O. Ogbobe, E. Oguzie, *International Journal of Applied Science and Engineering Research*, 3 (2014) 241-256.
17. I. Okechi Arukalam, I. Chimezie Madufor, O. Ogbobe, E. E. Oguzie, *Pigment & Resin Technology*, 43 (2014) 151-158.
18. J. Araki, *Soft Matter*, 9 (2013) 4125-4141.
19. L. Wu, J. Zhang, W. Watanabe, *Adv. Drug Delivery Rev.*, 63 (2011) 456-469.
20. S.C. Shi, C.C. Su, *Mater. Chem. Phys.*, 248 (2020) 122929.
21. S.C. Shi, *Sens. Mater.*, 31 (2019) 1599-1608.
22. M. Wang, L. Wang, Y. Huang, *J. Appl. Polym. Sci.*, 106 (2007) 2177-2184.
23. H.J. Park, G.H. Lee, J.-H. Jun, M. Son, Y.S. Choi, M.-K. Choi, M.J. Kang, *Carbohydr. Polym.*, 136 (2016) 692-699.
24. S.C. Shi, C.C. Su, *Materials*, 9 (2016) 612.
25. S. Tambe, S. Singh, M. Patri, D. Kumar, *Prog. Org. Coat.*, 72 (2011) 315-320.
26. S. Haruyama, M. Asari, T. Tsuru, *Corrosion protection by organic coatings*, (1987) United States.
27. S. Wang, A. Lu, L. Zhang, *Prog. Polym. Sci.*, 53 (2016) 169-206.
28. C.M. Gore, J.O. White, E.D. Wachsman, V. Thangadurai, *J. Mater. Chem. A*, 2 (2014) 2363-2373.
29. Q. Li, V. Thangadurai, *J. Mater. Chem.*, 20 (2010) 7970-7983.
30. Q. Li, V. Thangadurai, *Fuel Cells*, 9 (2009) 684-698.
31. E. Chinarro, J. Jurado, F. Figueiredo, J. Frade, *Solid State Ionics*, 160 (2003) 161-168.
32. P. Hjalmarsson, M. Søgaard, M. Mogensen, *Solid State Ionics*, 180 (2009) 1395-1405.
33. D. Phan, T. Häger, W. Hofmeister, *J. Raman Spectrosc.*, 48 (2017) 453-457.
34. M. Hanesch, *Geophys. J. Int.*, 177 (2009) 941-948.
35. S.C. Shi, T.W. Chang, *Opt. Quantum Electron.*, 50 (2018) 440.
36. S.C. Shi, T.W. Chang, *Opt. Quantum Electron.*, 50 (2018) 438.
37. I. Arukalam, I. Madufor, O. Ogbobe, E. Oguzie, *International Journal of Engineering and Technical Research*, 3 (2015) 163-169.